PCCP

RSC Publishing

PAPER

View Article Online
View Journal | View Issue

Published on 20 May 2013. Downloaded by Michigan State University on 20/01/2016 17:21:35.

Cite this: *Phys. Chem. Chem. Phys.*, 2013, **15**, 12694

Describing curved–planar π–π interactions: modeled by corannulene, pyrene and coronene†

Jiewei Li,[ab] Yuyu Liu,[a] Yan Qian,*[a] Lu Li,[a] Linghai Xie,*[ac] Jingzhi Shang,[b] Ting Yu,[b] Mingdong Yi[a] and Wei Huang*[ac]

Received 13th March 2013,
Accepted 17th May 2013

DOI: 10.1039/c3cp51095f

www.rsc.org/pccp

The specific π–π interactions between curved and planar structures, which are different from the general π–π interactions between planar arenes, have generated great attention due to their brand-new, unique, and fascinating photoelectric properties. Herein, the curved–planar (C–P) π–π interactions between corannulene, pyrene and coronene have been investigated using the DFT-D method. A series of structural and physical properties have been calculated including geometry, C–C distance, binding energy, population charge distribution, dipole moment, electrostatic potential (ESP), visualization of the interactions in real space, transfer integral, electronic transition behaviour and Raman shift. All the analyses indicate that the bowl–planar (C_B–P) complexes are distinguishable from the mouth-tip–planar (C_M–P) and planar–planar (P–P) packing motifs due to their coherent negative ESP, electronic attraction strength and Raman spectra. The C–P complexes are found to exhibit dominant electron transport characteristics. In addition, an unusual ''negative Stokes shift'' is found in the C–P π–π complexes, which is caused by state resonance. This provides a clue to help predict and explore the photoelectric properties of C–P π–π complexes. In particular, at the frequency of the out-of-plane CH bending vibration around 1400 cm^{-1}, the planar molecules in the C_B–P complexes possess a smaller Raman peak shift than in the C_M–P complexes, and *vice versa* for the curved molecules. This specific Raman shift can be utilized as characteristic signals to identify the C–P structures.

1. Introduction

π–π interactions between molecules have been of great importance for understanding the structure–property relationships of bio-systems,[1–3] supra-molecular chemistry[4–6] and self-assembly,[7] as well as organic nano-materials[8] and optoelectronic semiconductors, since supra-molecular chemistry was established by Lehn in 1987.[4,5] The π–π interactions are heavily related to the charge transfer between bases in DNA.[9–12] Furthermore, π–π interactions are one of the crucial driving forces in non-covalent synthesis, supra-molecular polymerizations and molecular self-assembly for constructing high-ordered superstructures such as aggregates and nano-structures.[13,14] In particular, controlling the π–π motifs in organic functional layers is a key technique to achieving high performance in organic devices.[15–17] In organic/polymer semiconductors, the multi-scale arrangement style of π-segments directly determines electronic processes such as carrier injection/transportation,[18–22] and exciton behaviors such as recombination/separation[23–25] and energy transfer.[26] As a result, polymer semiconductors are categorized into π-conjugated polymers and π-stacked polymers, which impart fundamentally different individual features when used for plastic electronics.[27,28] A deep investigation of π–π interactions is essential because understanding the structure-property relationships is crucial for improving the photoelectronic properties of organic functional materials,[29–33] and exploring further applications such as organic transistors[34,35] and π–π interaction driven DNA sequencing electronic devices.[36] To date, much effort has been made to improve the theoretical understanding of planar–planar (P–P) π–π interactions (sandwich, parallel displaced, T-shaped and Y-shaped packing motifs[31,37]) including the

[a] *Center for Molecular Systems and Organic Devices (CMSOD), Key Laboratory for Organic Electronics & Information Displays and Institute of Advanced Materials, Nanjing University of Posts & Telecommunications, Nanjing 210046, China. E-mail: iamwhuang@njupt.edu.cn, iamlhxie@njupt.edu.cn, iamyqian@njupt.edu.cn; Fax: +86 25-8586-6999; Tel: +86 25 8586 6008*

[b] *Division of Physics and Applied Physics, School of Physical and Mathematical Sciences, Nanyang Technological University, 637371, Singapore. Fax: +65 63167899; Tel: +65 63167899*

[c] *Jiangsu-Singapore Joint Research Center for Organic/Bio- Electronics & Information Displays and Institute of Advanced Materials, Nanjing University of Technology, Nanjing 211816, China*

† Electronic supplementary information (ESI) available: The visualization details of π–π interactions and UV/PL for C16–20(B) and C24–20(B) complexes. See DOI: 10.1039/c3cp51095f

This journal is © the Owner Societies 2013

Published on 20 May 2013. Downloaded by Michigan State University on 20/01/2016 17:21:35.

configurations, interaction distance, transfer integral, binding energy, *etc.*, which provide rational guides for experimental investigations.[33,38–44]

In recent years, the specific π–π interactions between curved and planar structures have generated great attention due to their brand-new, unique, and fascinating photoelectric properties, which show great potential for a wide variety of applications.[45–47] Since the well known curved corannulenes were first synthesized by Barth and Lawton in 1966,[48,49] many experimental and theoretical works have been conducted to explore their peculiar properties,[50–57] which include ion/molecule reactions,[58] host-guest interactions and co-crystallization,[59] self-assembly of a 1D non-covalent metal–organic nanowire,[60] anion mediated structural motifs,[61] and highly charged corannulenes.[62,63] For example, Petrukhina's group found, using crystal data, that a curve can be induced into the planar [Hg_3] molecule when it interacts with the curved corannulene leading to a Hg–C distance of about 3.0 Å, which is the shortest contact length observed in organo-mercurial complexes.[64,65] It is anticipated that some of their unique properties are related to their curved hexagon or hybrid hexagon–pentagon structures.[45–47] Therefore, interactions between planar and curved molecules have generated considerable interest in materials chemistry[66] to help better understand the molecular/supra-molecular properties[64,67] and furthermore, the "bulk" opto-electrical properties. However, to the best of our knowledge, systematic theoretical investigations from structure to properties, concerning the comparison of the C–P π–π interactions in corannulene-based complex with the corresponding P–P π–π interactions, have not been reported yet. Therefore, theoretical investigations on such topics are vital to understand the C–P π–π interactions of the corannulene-based complex. Herein, pyrene and coronene are selected as planar molecules for the systematic theoretical investigation of corannulene-based C–P complexes (see Fig. 1), taking into consideration the highly symmetric geometries, similar carbon numbers, as well as the vastly investigated functionalities of all three components.[68,69] For simplicity, we have denoted corannulene, pyrene and coronene as C20, C16 and C24, respectively, according to the number of carbon atoms they possess. Various π–π interactions were formed between the three molecules, and their corresponding properties have been calculated.

As density function theory (DFT) including an empirical van der Waals correction of the form R^{-6} (DFT-D) can describe long range interactions accurately,[56,70–73] B97D can be used to obtain the best results for the corannulene system.[74] Thus, in the present work, B97D was implemented to investigate the geometric optimization, binding energy, population charge distribution, dipole moment and electrostatic potential (ESP) using the Gaussian09 program.[75] The excitation energies of the ground and excited state, which directly correlate to their photo-physical behaviors, were calculated using the TD-B97D method. Based on the wave function generated by Gaussian09, transfer integrals were calculated and the visualization of the weak interactions in real space have been performed using Multiwfn 2.6 software.[76] These theoretical descriptions give a significant insight into uncovering and predicting the photoelectric properties of the C–P π–π interactions. Finally, GGA-PBE including a TS correction[77] was implemented to calculate the Raman spectra in the Material Studio Dmol3 module. The result of the Raman analysis suggests that the P–P π–π interactions display a red shift. In addition, due to the C–P π–π interactions, the frequency of the out-of-plane CH bending vibration around 1400 cm^{-1} of the planar molecules in the C_B–P complexes exhibit a smaller shift than in the C_M–P complexes, but the vibrations of the curved molecules exhibit a larger shift. This specific Raman shift can be utilized as a characteristic signal to distinguish between C–P structures in the fields of supra-molecular chemistry and materials chemistry.

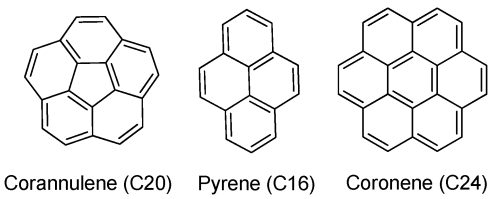

Fig. 1 Molecular structures of C20, C16 and C24.

2. Computational details

The ground state geometrical structures were fully optimized using the B97D method[70,71,74] at the TZVP level. The energies, dipole moments and population charge distributions were then calculated by the same method using the Gaussian09 program. The excited states were optimized at the TD-B97D/6-31G(D) level. The absorption and emission spectra were systematically investigated using TD-B97D/TZVP based on the optimized structures. GGA-PBE was implemented to calculate the Raman spectra in the Material Studio 6.0 Dmol3 module with the DNP 4.4 basis including TS correction,[77] core electron was treated using an All Electron Relativistic, and all of the parameters are fine (PBE0-TS method has been previously reported.[73] Here we used the PBE-TS method based on the good similarity between the calculated Raman peak wavelength of C20 (1435 cm^{-1}) and the experimental data (1429 cm^{-1}),[78] which is attributed to the out-of-plane CH bending vibration). The transfer integrals were calculated *via* the direct method[79] based on the wave function generated by Gaussian09 at the B97D/TZVP level. The visualization of weak interactions was conducted using Multiwfn 2.6 software[76] in real space (ESI,† Fig. S1). The graphic displays of π–π interactions were then drawn using VMD 1.9 [http://www.ks.uiuc.edu/]. This visualization method was successfully and widely used in many other works.[80,81]

3. Results and discussion

Firstly, the dimers/complex of C16–16, C16–24 and C24–24, which are induced by P–P π–π interactions, were fully optimized at the B97D/TZVP level (see Fig. 2). C16–16 is parallel stacked and is similar to the crystal structure of Pyrene03[82] in the Cambridge Crystallographic Data Centre (CCDC). The shortest C–C distance between two monomers in the C16–16 dimer is

Published on 20 May 2013. Downloaded by Michigan State University on 20/01/2016 17:21:35.

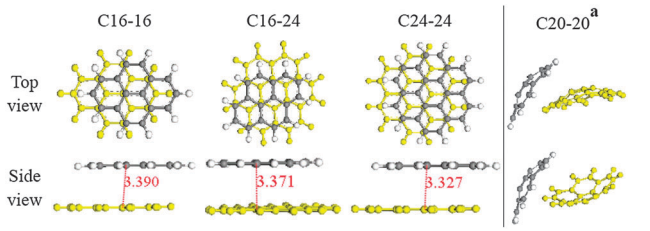

Fig. 2 Geometrical configurations of P–P and curved–curved dimer/complex. [a] Listing the two stable configurations of C20–20 selected from CCDC: M–B (up) and M–M (down, more stable).

calculated to be ~3.39 Å, close to the value from the crystal structure (3.47 Å), which verifies the accuracy of the B97D method.[72,74] The most stable configuration of C24–24 has staggered stacking, similar to the previously reported theoretical results[37] and slightly different from the parallel stacking seen in the crystal structures. The distance between two parallel monomer planes of C16–24 is ~3.37 Å, a bit shorter than that of C16–16 (3.39 Å), but longer than that of the C24–24 dimer (3.33 Å). The plane distances of all the three reported C24 crystals are ~3.46 Å, ~3.39 Å and ~3.46 Å,[83–85] respectively, close to our calculated value of ~3.33 Å.

Analysis was then conducted based on the three curved–curved configurations of $C20_{M-M}$ (mouth-tip to mouth-tip), $C20_{M-B}$ (mouth-tip to bowl) and $C20_{B-B}$ (bowl to bowl) dimers, which were directly obtained from the CCDC. The M–M and M–B (Fig. 2, right side) are more stable than B–B configuration with total energies of −41781.23 eV, −41781.35 eV and −41781.02 eV, respectively. Finally, for the C–P interaction, the four C–P configurations of the C16–20(B), C24–20(B), C16–20(M) and C24–20(M) complexes (Fig. 3) were optimized, which were all found to possess quasi-parallel stacking. The minimum C–C distances of the C_B–P complexes are shorter than those of the C_M–P and P–P configurations. The minimum C–C distances of C16–20(B) and C16–20(M) are ~3.11 Å and ~3.35Å, respectively, while those of C24–20(B) and C24–20(M) complexes are ~3.09 Å and ~3.26 Å, respectively. For the P–P configurations, the minimum C–C distances of C16–16, C16–24 and C24–24 are ~3.39 Å, ~3.37 Å and ~3.33 Å, respectively. As expected, all the planar molecules in the C–P complexes become a little curved as a result of C–P π–π interactions, which is similar to the previously reported works.[64,65]

As shown in Table 1, the total binding energy of C24–C24 is ~0.985 eV, which is similar to other prior works.[37,71] The binding energy per carbon atom for C16–16, C16–20(B), C16–20(M), C16–24, C24–20(B), C24–20(M) and C24–24 are 0.018, 0.016, 0.018, 0.019, 0.021, 0.017 and 0.017 eV, respectively. The C_B–P complexes have smaller binding energies than the C_M–P and P–P complexes, probably due to the longer distances and weaker interactions between the edge carbon atoms of the B (C20) and P (C16/C24) planes. In general, binding energies of the C–P complexes are smaller than the P–P ones, which means that the π–π interactions of the C–P complexes are weaker than the P–P ones.

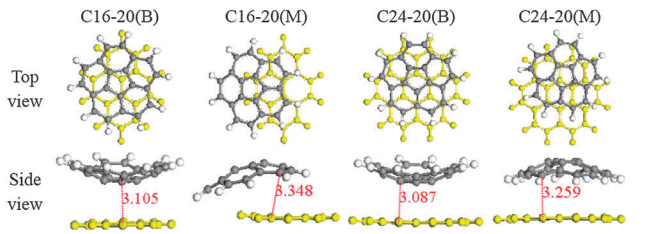

Fig. 3 Geometrical configurations of the C–P π–π complexes.

Table 1 Total binding energy of the dimer/complex and binding energy of an average carbon atom

	C16–16	C16–20(B)	C16–20(M)	C16–24	C24–24	C24–20(B)	C24–20(M)
Total (eV)	0.573	0.560	0.651	0.755	0.985	0.761	0.750
Average (eV)	0.018	0.016	0.018	0.019	0.021	0.017	0.017

In Fig. 4, the population charge distributions (analyzed using the NBO method) and dipole moments show that there is almost no electron transfer or change in the dipole moments of the C16–16 and C24–24 dimers, indicating that the π–π interactions in the C16–16 and C24–24 dimers are dominated by electron dispersion forces. However, the C16–24 complex displays an extra local dipole–dipole effect, with a significant change in dipole moment of 0.34 Debye. The C_B–P configurations have an effective charge transfer from the planar molecule to the curved molecule, with the values for the C16–20 and C24–20 complexes being 0.02 e and 0.03 e, respectively. This charge transfer is probably because of the strong anionic attraction of corannulene[62] and the negative electrostatic potential at the bowl bottom.[86] Furthermore, a change in dipole moment is also found in the C_B–P configurations. The simultaneous charge transfer and dipole moment change are different from a pentacene–fullerene complex,[67] which has only a change in dipole moment, but no charge transfer. C_M–P configurations only have the dipole moment alteration, which is smaller than that of the C_B–P ones. The electrostatic potential analysis shows that the C_B–P interactions between monomers have a coherent negative electrostatic potential, while the P–P and C_M–P interactions have an incoherent or coherent positive electrostatic potential, which is consistent with the analysis of the population charge distribution and dipole moment. This indicates that the C_B–P interactions are distinguishable from the C_M–P and P–P interactions.

The visualization of the π–π interactions between the two monomers in real space were drawn using VMD software with a scale running from −0.015 (min) to 0.015 (max), as shown in Fig. 5. The results reveal that the P–P π–π interactions have a continuous wave function overlap with a very weak electronic attraction effect. The C_B–P interactions have a discontinuous wave function overlap, but a strong electronic attraction effect, which is probably due to the charge transfer and change in dipole moment that is mentioned above. C_M–P interactions have a discontinuous wave function overlap and an almost dominant van der Walls effect. The fantastic electronic attraction effect of the C_B–P interactions correlated well with the above population charge distribution and the ESP analysis.

From Marcus Theory, it is well known that the transfer integral is one of the most important parameters for carrier

 This journal is © the Owner Societies 2013

Published on 20 May 2013. Downloaded by Michigan State University on 20/01/2016 17:21:35.

	C16-16	C16-20(B)	C16-20(M)	C16-24	C24-24	C24-20(B)	C24-20(M)
NBO[a]	0.00	-0.017	0.001	0.001	0.00	-0.025	0.002
DM	0.00[b] 0.00[c]	0.00 2.23	0.00 2.23	0.00 0.00	0.00 0.00	0.00 2.23	0.00 2.23
	0.00[d]	1.95	2.08	0.34	0.00	1.83	2.51
ESP	-0.01						0.01

Fig. 4 Summary of the population charge distributions (NBO), dipole moments (DM) (Debye) and electrostatic potential (ESP). [a] The charge of the latter monomer in the dimer/complex (units: e). [b,c] The original dipole moment of the former and latter monomer, respectively. [d] Total dipole moment of the dimer/complex.

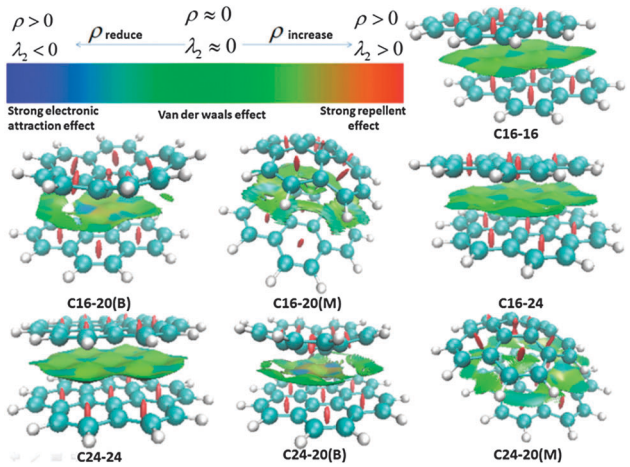

Fig. 5 Visualization of the weak interactions in real space. The scale runs from −0.015 (min) to 0.015 (max).

mobility in organic electronic materials.[87] The transfer integral is mainly determined by the frontier orbital coupling of adjacent monomers,[88] where the HOMO and LUMO coupling correspond to the hole (t_h) and electron (t_e) transfer integral, respectively. The transfer integral between the two monomers in the dimers/complexes have been calculated using the direct method[79] in order to understand the carrier transporting characteristics of the various π–π interactions. The results are summarized in Table 2 and Fig. S3 (ESI†), and consider the relative degenerate/near-degenerate orbitals. The hole (t_h = 115 meV) and electron (t_e = 124 meV) transfer integrals of C16–16 are comparable.

Table 2 The hole (t_h) and electron (t_e) transfer integrals between the two monomers in a dimer/complex (units: meV). The HOMO (LUMO) of C16, C20, C24 are 53 (54), 65 (66) and 78 (79), respectively

	C16–16	C16–20(B)	C16–20(M)	C16–24	C24–24	C24–20(B)	C24–20(M)
t_h	115	30	11	185	187	32	74
t_e	124	136	49	159	135	81	139

For C16–24 and C24–24, t_h is much bigger than t_e. The value of t_h for C16–24 and C24–24 are 185 and 187 meV, respectively, while the values of t_e are 159 and 135 meV, respectively. However, for the C–P complexes, the value of t_e is much bigger than t_h, which indicates that the C–P complexes are prospective candidates for n-type optoelectronic materials. The values of t_h for C16–20(B), C16–20(M), C24–20(B) and C24–20(M) are 30, 11, 32 and 74 meV, respectively, while the t_e value are 136, 49, 81 and 139 meV, respectively. The difference in the charge transport characteristics between the C–P and P–P complexes are attributed to the strong electronic attraction ability of corannulene,[62] which is consistent with the population charge distribution analysis discussed above.

In addition, supra-molecular π–π interactions are vital to affect the condensed-state photophysical behaviors of organic functional materials, which directly determines their fantastic characteristics such as organic solid-state laser emission, aggregation induced emission, β-phase emission and so on.[89–92] To date, deep investigations of these supra-molecular π–π interactions, concerning theoretical works, are still limited.[93,94] In this work, the absorption (UV-vis) and photoluminescence (PL) spectra have been calculated using TD-B97D at the TZVP level. The maximum fluorescence emission peak of the C16–16 dimer is calculated to be 380.86 nm, attributable to the intrinsic pyrene emission and very close to the reported experimental value of 375 nm.[95] Similar to most of the organic systems, the C_M–P complexes display a positive Stokes shift due to vibrational relaxation (Fig. 6 and Table 3). However, as shown in Fig. 6a, it is surprising to find that C16–20(B) has an abnormal "negative Stokes shift",[96] and a specific PL enhancement. For clarified discussion, the electronic transition parameters of C–P complexes are summarized in Table 3. The results show that both the main UV and PL peaks of C_B–P contain several transitions which are close to each other (Fig. S2, ESI†). The maximum absorption peak of C16–20(B) is 386.55 nm with an oscillator strength of f = 0.028 which is attributed to the HOMO → LUMO + 2 transition from the S_0 to S_7 state. Surprisingly, the maximum fluorescence emission peak around 383.73 nm, attributable to the LUMO + 2 → HOMO transition from the S_9 to S_0 state, is an

Published on 20 May 2013. Downloaded by Michigan State University on 20/01/2016 17:21:35.

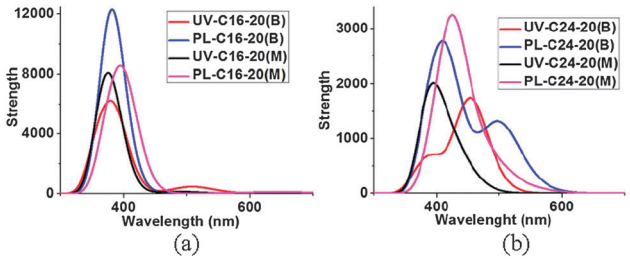

Fig. 6 Absorption (UV) and photoluminescence emission (PL) spectra of C16–20 (a) and C24–20 (b) C–P complexes.

Table 3 Absorption and emission spectra in vacuum obtained using TD-B97D/TZVP. H denotes the HOMO, and L the LUMO

	Electronic transitions	λ^{abs} (nm) / λ^{em} (nm)	f^{abs} / f^{em}	Main configurations	
C16–20(B)	$S_0 \rightarrow S_{12}$	364.05	0.017	H − 4 → L	25%
				H − 3 → L + 1	41%
	$S_0 \rightarrow S_{11}$	365.92	0.010	H − 5 → L	24%
	$S_0 \rightarrow S_{10}$	371.56	0.011	H − 2 → L + 2	30%
	$S_0 \rightarrow S_7$	386.55	0.028	H → L + 2	27%
	$S_0 \rightarrow S_6$	391.35	0.022	H − 2 → L + 1	24%
				H − 2 → L + 2	15%
	$S_{11} \rightarrow S_0$	370.40	0.030	L + 1 → H − 5	46%
	$S_9 \rightarrow S_0$	383.73	0.102	L + 2 → H − 2	19%
				L + 2 → H	60%
	$S_7 \rightarrow S_0$	395.70	0.030	L + 2 → H − 2	52%
C16–20(M)	$S_0 \rightarrow S_{12}$	366.10	0.046	H − 4 → L + 2	41%
	$S_0 \rightarrow S_8$	383.21	0.058	H → L + 2	53%
	$S_{12} \rightarrow S_0$	377.41	0.034	L + 1 → H − 5	34%
				L → H − 4	41%
	$S_7 \rightarrow S_0$	400.41	0.061	L + 1 → H − 2	21%
				L + 2 → H	52%
	$S_6 \rightarrow S_0$	409.51	0.023	L + 1 → H − 2	66%
C24–20(B)	$S_0 \rightarrow S_{15}$	369.25	0.004	H − 5 → L	52%
	$S_0 \rightarrow S_{10}$	393.70	0.005	H − 2 → L + 2	84%
	$S_0 \rightarrow S_4$	453.01	0.017	H − 1 → L	28%
				H − 1 → L + 1	15%
				H → L + 1	55%
	$S_{15} \rightarrow S_0$	386.71	0.015	L → H − 4	52%
	$S_{10} \rightarrow S_0$	415.17	0.012	L + 2 → H − 2	55%
				L + 2 → H	19%
	$S_8 \rightarrow S_0$	424.37	0.014	L + 2 → H	51%
	$S_2 \rightarrow S_0$	504.43	0.010	L → H − 1	90%
C24–20(M)	$S_0 \rightarrow S_{15}$	382.52	0.004	H − 3 → L + 3	71%
	$S_0 \rightarrow S_{14}$	387.15	0.009	H − 4 → L + 1	31%
	$S_0 \rightarrow S_{12}$	391.80	0.006	H − 5 → L	33%
				H − 3 → L + 2	16%
	$S_{14} \rightarrow S_0$	394.64	0.008	L + 1 → H − 4	44%
	$S_{10} \rightarrow S_0$	425.07	0.033	L + 1 → H − 2	26%
				L + 2 → H	34%

abnormal negative Stokes shift (blue shift) and possesses a larger oscillator strength (f = 0.102) compared to the absorption (386.55 nm, f = 0.028). This specific negative Stokes shift and enhancement of the emission are probably caused by the state resonance[97,98] between S_{10} and S_7 (Fig. 7a), which can be explained by two factors. On the one hand, the absorption

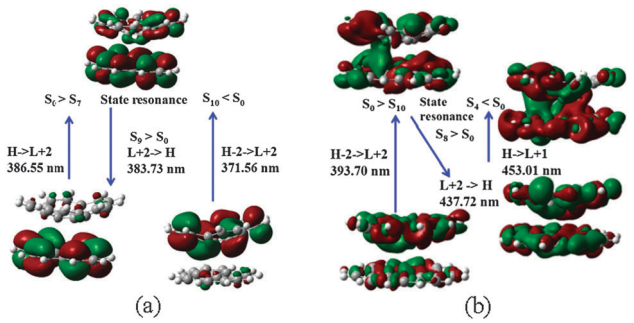

Fig. 7 The main electronic transition state-resonance behavior of the C_B–P complexes. (a): C16–20(B); (b): C24–20(B).

from S_0 to S_{10} (corresponding to the HOMO − 2 → LUMO + 2 transition) has the same terminal excited state as the absorption from S_0 to S_7 (corresponding to the HOMO → LUMO + 2 transition). On the other hand, the vertical transition energies of $S_0 \rightarrow S_{10}$ (3.34 eV) and $S_0 \rightarrow S_7$ (3.21 eV) are quite similar, with only a 0.13 eV difference.

In the C24–20(B) complex, shown in Fig. 6b and 7b, a similar state resonance and corresponding "enhanced" fluorescence emission at the high energy peak occur. The strongest high energy absorption peak around 393.70 nm is attributed to the HOMO − 2 → LUMO + 2 transition from S_0 to S_{10} with an oscillator strength of f = 0.005. While the high energy emission peak is attributed to the LUMO + 2 → HOMO transition from S_8 to S_0 state with an oscillator strength of f = 0.014. The "enhanced emission" is probably caused by the state resonance between the S_{10} and S_4 states, with a difference of only 0.41 eV in their vertical transition energies, as the absorption from the S_0 to S_4 state is mainly from the HOMO → LUMO + 1 transition (f = 0.017). This unique fluorescence emission enhancement of C_B–P π–π interactions may be utilized in bio-imaging, environmental detection and materials science.[92,99–101]

Furthermore, we calculated the Raman spectra in order to gain insight into the C–P π–π interactions. Raman spectral characterization is a very powerful tool for investigating π–π interactions such as the photo-switching between azobenzene and graphene,[102] crystalline phase or supra-molecular structure confirmation[103,104] and excited-state π–π interactions.[105] The calculated results, analyzed at 298.0 K with an incident light of 514.5 nm (smearing = 10 cm^{-1}), are shown in Fig. 8 and Fig. S4 and S5 (ESI†). The strongest out-of-plane CH bending vibration,

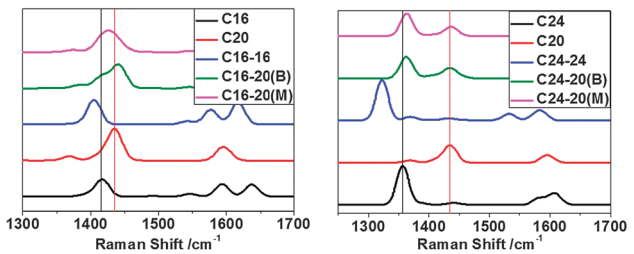

Fig. 8 The calculated Raman spectra for the out-of plane vibrations of the carbon skeleton for the monomers, C–P and P–P dimer/complexes.

 This journal is © the Owner Societies 2013

Published on 20 May 2013. Downloaded by Michigan State University on 20/01/2016 17:21:35.

at around 1400 cm^{-1}, was selected for the investigation because of its high sensitivity to the π electrons.[104] The Raman shift became larger with an increasing number of π electrons with the shift values of C16–16 and C24–24 being −12.4 cm^{-1} and −34.6 cm^{-1}, respectively. In this work, the P–P π–π interactions exhibit a red Raman shift when compared with their monomer, while the C–P π–π interactions mostly exhibit a blue Raman shift. Induced by the C–P π–π interactions, the planar molecules in the C_B–P complexes possess a smaller peak shift than the C_M–P complexes and *vice versa* for the curved molecules. For the planar molecules in the C16–20(B), C16–20(M), C24–20(B) and C24–20(M) complexes, the Raman shifts are 1.6, 6.2, 5.4 and 6.4 cm^{-1}, respectively. For the curved molecules, the corresponding Raman shifts are 4.4, −0.5, 1.1 and 0.3 cm^{-1}, respectively. This specific Raman shift can be utilized as a characteristic signal to help distinguish and identify the C–P structures in the fields of supra-molecular chemistry and materials chemistry.

4. Conclusions

In summary, the C–P π–π interaction is likely to induce quasi-parallel stacking, similar to the P–P stacking. The C_B–P complexes have the shortest C–C bond distance of ∼3.1 Å. Binding energy per carbon atom of the C–P complexes is smaller than for the P–P dimers/complexes. The C_B–P complexes possess an effective charge transfer, a change in their dipole moment, a coherent negative ESP and a strong electronic attraction effect, which can be used to distinguish them from C_M–P and P–P structures. The C–P complexes are found to exhibit dominant electron transport abilities. As for their optical properties, the maximum emissions of the C_B–P complexes are enhanced and display a unique "negative Stokes shift", which is due to the state resonance between the high and low energy states. This gives an insight into uncovering and predicting the photoelectric properties of C–P complexes. Furthermore, C–P complexes exhibit specific Raman shifts at the frequency of the out-of-plane CH bending vibration around 1400 cm^{-1}, which can be utilized to identify the C–P structures. These investigations of C–P π–π interactions provide a valuable guide for experimental research.

Acknowledgements

We thank Prof. Yuanping Yi from Institute of Chemistry, Chinese Academy of Sciences for helping us with the calculation of the transfer integrals. We thank the National Basic Research Program of China (2009CB930601), National Natural Science Foundation of China (21003706, 21274064, 21144004, 60876010, 61177029, 20774043, 20704023, and 20974046), the Program for New Century Excellent Talents in University (NCET-11-0992), and Program for Postgraduates Research Innovation in University of Jiangsu Province (CXLX11_0410, CXLX11_0413, CXLX11_0422, CXLX11_0423). L. H. X. thanks Jiangsu Overseas Research & Training Program for University Prominent Young & Middle-aged Teachers and Presidents.

References

1 R. Hoffmann, *Acc. Chem. Res.*, 1971, **4**, 1–9.
2 D. N. Beratan, J. N. Betts and J. N. Onuchic, *Science*, 1991, **252**, 1285–1288.
3 T. R. Prytkova, I. V. Kurnikov and D. N. Beratan, *Science*, 2007, **315**, 622–625.
4 E. A. Meyer, R. K. Castellano and F. Diederich, *Angew. Chem., Int. Ed.*, 2003, **42**, 1210–1250.
5 M. W. Hosseini, J. M. Lehn, L. Maggiora, K. B. Mertes and M. P. Mertes, *J. Am. Chem. Soc.*, 1987, **109**, 537–544.
6 J.-M. Lehn, *Angew. Chem., Int. Ed.*, 1988, **27**, 89–112.
7 V. Georgakilas, M. Otyepka, A. B. Bourlinos, V. Chandra, N. Kim, K. C. Kemp, P. Hobza, R. Zboril and K. S. Kim, *Chem. Rev.*, 2012, **112**, 6156–6214.
8 J. Y. Lee, B. H. Hong, W. Y. Kim, S. K. Min, Y. Kim, M. V. Jouravlev, R. Bose, K. S. Kim, I.-C. Hwang, L. J. Kaufman, C. W. Wong, P. Kim and K. S. Kim, *Nature*, 2009, **460**, 498–501.
9 G. B. Schuster, *Acc. Chem. Res.*, 2000, **33**, 253–260.
10 F. D. Lewis, R. L. Letsinger and M. R. Wasielewski, *Acc. Chem. Res.*, 2001, **34**, 159–170.
11 M. A. O'Neil and J. K. Barton, *J. Am. Chem. Soc.*, 2004, **126**, 11471–11483.
12 R. E. Holmlin, P. J. Dandliker and J. K. Barton, *Angew. Chem., Int. Ed.*, 1997, **36**, 2714–2730.
13 T. F. A. De Greef, M. M. J. Smulders, M. Wolffs, A. P. H. J. Schenning, R. P. Sijbesma and E. W. Meijer, *Chem. Rev.*, 2009, **109**, 5687–5754.
14 A. D'Urso, M. E. Fragala and R. Purrello, *Chem. Commun.*, 2012, **48**, 8165–8176.
15 J. L. Segura, N. Martin and D. M. Guldi, *Chem. Soc. Rev.*, 2005, **34**, 31–47.
16 A. J. Mayne, G. Dujardin, G. Comtet and D. Riedel, *Chem. Rev.*, 2006, **106**, 4355–4378.
17 T. W. Holcombe, J. E. Norton, J. Rivnay, C. H. Woo, L. Goris, C. Piliego, G. Griffini, A. Sellinger, J.-L. Brédas, A. Salleo and J. M. J. Fréchet, *J. Am. Chem. Soc.*, 2011, **133**, 12106–12114.
18 Y. Sun, Y. Liu and D. Zhu, *J. Mater. Chem.*, 2005, **15**, 53–65.
19 P. Prins, K. Senthilkumar, F. C. Grozema, P. Jonkheijm, A. P. H. J. Schenning, E. W. Meijer and L. D. A. Siebbeles, *J. Phys. Chem. B*, 2005, **109**, 18267–18274.
20 A. Saeki, Y. Koizumi, T. Aida and S. Seki, *Acc. Chem. Res.*, 2012, **45**, 1193–1202.
21 Y. Che, A. Datar, X. Yang, T. Naddo, J. Zhao and L. Zang, *J. Am. Chem. Soc.*, 2007, **129**, 6354–6355.
22 R. J. Chesterfield, J. C. McKeen, C. R. Newman, P. C. Ewbank, D. A. da Silva Filho, J.-L. Brédas, L. L. Miller, K. R. Mann and C. D. Frisbie, *J. Phys. Chem. B*, 2004, **108**, 19281–19292.
23 M. R. Wasielewski, *Acc. Chem. Res.*, 2009, **42**, 1910–1921.
24 J.-L. Brédas, D. Beljonne, V. Coropceanu and J. Cornil, *Chem. Rev.*, 2004, **104**, 4971–5004.
25 F. J. M. Hoeben, P. Jonkheijm, E. W. Meijer and A. P. H. J. Schenning, *Chem. Rev.*, 2005, **105**, 1491–1546.

Published on 20 May 2013. Downloaded by Michigan State University on 20/01/2016 17:21:35.

26 J. Vura-Weis, S. H. Abdelwahed, R. Shukla, R. Rathore, M. A. Ratner and M. R. Wasielewski, *Science*, 2010, **328**, 547–1550.
27 L.-H. Xie, Q.-D. Ling, X.-Y. Hou and W. Huang, *J. Am. Chem. Soc.*, 2008, **130**, 2120–2121.
28 L.-H. Xie, C.-R. Yin, W.-Y. Lai, Q.-L. Fan and W. Huang, *Prog. Polym. Sci.*, 2012, **37**, 1192–1264.
29 V. Coropceanu, T. Nakano, N. E. Gruhn, O. Kwon, T. Yade, K.-i. Katsukawa and J.-L. Brédas, *J. Phys. Chem. B*, 2006, **110**, 9482–9487.
30 G. C. Solomon, J. Vura-Weis, C. Herrmann, M. R. Wasielewski and M. A. Ratner, *J. Phys. Chem. B*, 2010, **114**, 14735–14744.
31 T. F. Headen, C. A. Howard, N. T. Skipper, M. A. Wilkinson, D. T. Bowron and A. K. Soper, *J. Am. Chem. Soc.*, 2010, **132**, 5735–5742.
32 W. Pisula, X. Feng and K. Müllen, *Adv. Mater.*, 2010, **22**, 3634–3649.
33 T. S. Totton, A. J. Misquitta and M. Kraft, *J. Chem. Theory Comput.*, 2010, **6**, 683–695.
34 W. H. Lee, J. Park, S. H. Sim, S. Lim, K. S. Kim, B. H. Hong and K. Cho, *J. Am. Chem. Soc.*, 2011, **133**, 4447–4454.
35 W. H. Lee, J. Park, S. H. Sim, S. B. Jo, K. S. Kim, B. H. Hong and K. Cho, *Adv. Mater.*, 2011, **23**, 1752–1756.
36 S. K. Min, W. Y. Kim, Y. Cho and K. S. Kim, *Nat. Nanotechnol.*, 2011, **6**, 162–165.
37 C. Feng, C. S. Lin, W. Fan, R. Q. Zhang and M. A. Van Hove, *J. Chem. Phys.*, 2009, **131**, 194702–194708.
38 A. Rochefort, R. Martel and P. Avouris, *Nano Lett.*, 2002, **2**, 877–880.
39 J. G. Hill, J. A. Platts and H.-J. Werner, *Phys. Chem. Chem. Phys.*, 2006, **8**, 4072–4078.
40 M. Piacenza and S. Grimme, *ChemPhysChem*, 2005, **6**, 1554–1558.
41 X. Feng, V. Marcon, W. Pisula, M. R. Hansen, J. Kirkpatrick, F. Grozema, D. Andrienko, K. Kremer and K. Mullen, *Nat. Mater.*, 2009, **8**, 421–426.
42 E. C. Lee, D. Kim, P. Jurečka, P. Tarakeshwar, P. Hobza and K. S. Kim, *J. Phys. Chem. A*, 2007, **111**, 3446–3457.
43 K. S. Kim, P. Tarakeshwar and J. Y. Lee, *Chem. Rev.*, 2000, **100**, 4145–4186.
44 N. J. Singh, S. K. Min, D. Y. Kim and K. S. Kim, *J. Chem. Theory Comput.*, 2009, **5**, 515–529.
45 X. Lu and Z. Chen, *Chem. Rev.*, 2005, **105**, 3643–3696.
46 A. Sygula, F. R. Fronczek, R. Sygula, P. W. Rabideau and M. M. Olmstead, *J. Am. Chem. Soc.*, 2007, **129**, 3842–3843.
47 L. Kobryn, W. P. Henry, F. R. Fronczek, R. Sygula and A. Sygula, *Tetrahedron Lett.*, 2009, **50**, 7124–7127.
48 W. E. Barth and R. G. Lawton, *J. Am. Chem. Soc.*, 1966, **88**, 80–381.
49 R. G. Lawton and W. E. Barth, *J. Am. Chem. Soc.*, 1971, **93**, 1730–1745.
50 Y.-T. Wu and J. S. Siegel, *Chem. Rev.*, 2006, **106**, 4843–4867.
51 A. M. Orendt, J. C. Facelli, S. Bai, A. Rai, M. Gossett, L. T. Scott, J. Boerio-Goates, R. J. Pugmire and D. M. Grant, *J. Phys. Chem. A*, 1999, **104**, 149–155.
52 A. S. Filatov, L. T. Scott and M. A. Petrukhina, *Cryst. Growth Des.*, 2010, **10**, 4607–4621.
53 T. J. Seiders, K. K. Baldridge, G. H. Grube and J. S. Siegel, *J. Am. Chem. Soc.*, 2001, **123**, 517–525.
54 A. Pogoreltsev, E. Solel, D. Pappo and E. Keinan, *Chem. Commun.*, 2012, **48**, 5425–5427.
55 I. V. Kuvychko, S. N. Spisak, Y.-S. Chen, A. A. Popov, M. A. Petrukhina, S. H. Strauss and O. V. Boltalina, *Angew. Chem., Int. Ed.*, 2012, **51**, 4939–4942.
56 D. Josa, J. R. Otero and E. M. C. Lago, *Phys. Chem. Chem. Phys.*, 2011, **13**, 21139–21145.
57 A. Tkatchenko, D. Alfè and K. S. Kim, *J. Chem. Theory Comput.*, 2012, **8**, 4317–4322.
58 H. Becker, G. Javahery, S. Petrie, P. C. Cheng, H. Schwarz, L. T. Scott and D. K. Bohme, *J. Am. Chem. Soc.*, 1993, **115**, 11636–11637.
59 L. N. Dawe, T. A. AlHujran, H.-A. Tran, J. I. Mercer, E. A. Jackson, L. T. Scott and P. E. Georghiou, *Chem. Commun.*, 2012, **48**, 5563–5565.
60 B. Topolinski, B. M. Schmidt, M. Kathan, S. I. Troyanov and D. Lentz, *Chem. Commun.*, 2012, **48**, 6298–6300.
61 E. L. Elliott, G. A. Hernandez, A. Linden and J. S. Siegel, *Org. Biomol. Chem.*, 2005, **3**, 407–413.
62 D. Eisenberg, J. M. Quimby, E. A. Jackson, L. T. Scott and R. Shenhar, *Chem. Commun.*, 2010, **46**, 9010–9012.
63 D. Eisenberg, J. M. Quimby, L. T. Scott and R. Shenhar, *J. Phys. Org. Chem.*, 2013, **26**, 124–130.
64 A. S. Filatov, E. A. Jackson, L. T. Scott and M. A. Petrukhina, *Angew. Chem., Int. Ed.*, 2009, **48**, 8473–8476.
65 A. S. Filatov, A. K. Greene, E. A. Jackson, L. T. Scott and M. A. Petrukhina, *J. Organomet. Chem.*, 2011, **696**, 2877–2881.
66 P. D. W. Boyd and C. A. Reed, *Acc. Chem. Res.*, 2005, **38**, 235–242.
67 M. Linares, D. Beljonne, J. r. m. Cornil, K. Lancaster, J.-L. Brédas, S. Verlaak, A. Mityashin, P. Heremans, A. Fuchs, C. Lennartz, J. Idé, R. l. Méreau, P. Aurel, L. Ducasse and F. d. r. Castet, *J. Phys. Chem. C*, 2010, **114**, 3215–3224.
68 T. M. Figueira-Duarte and K. Müllen, *Chem. Rev.*, 2011, **111**, 7260–7314.
69 U. Rohr, P. Schlichting, A. Böhm, M. Gross, K. Meerholz, C. Bräuchle and K. Müllen, *Angew. Chem., Int. Ed.*, 1998, **37**, 1434–1437.
70 S. Grimme, *J. Comput. Chem.*, 2006, **27**, 1787–1799.
71 S. Grimme and C. Mück-Lichtenfeld, *J. Phys. Chem. C*, 2007, **111**, 11199–11207.
72 M. P. Waller, H. Kruse, C. Muck-Lichtenfeld and S. Grimme, *Chem. Soc. Rev.*, 2012, **41**, 3119–3128.
73 Y. Cho, S. K. Min, J. Yun, W. Y. Kim, A. Tkatchenko and K. S. Kim, *J. Chem. Theory Comput.*, 2013, **9**, 2090–2096.
74 R. Peverati and K. K. Baldridge, *J. Chem. Theory Comput.*, 2008, **4**, 2030–2048.
75 M. J. T. G. W. Frisch, H. B. Schlegel, G. E. Scuseria, M. A. Robb, J. R. Cheeseman, G. Scalmani, V. Barone, B. Mennucci, G. A. Petersson, H. Nakatsuji, M. Caricato, X. Li, H. P. Hratchian, A. F. Izmaylov, J. Bloino, G. Zheng, J. L. Sonnenberg, M. Hada, M. Ehara, K. Toyota, R. Fukuda, J. Hasegawa, M. Ishida, T. Nakajima, Y. Honda, O. Kitao,

 This journal is © the Owner Societies 2013

Published on 20 May 2013. Downloaded by Michigan State University on 20/01/2016 17:21:35.

H. Nakai, T. Vreven, J. A. Montgomery Jr., J. E. Peralta, F. Ogliaro, M. Bearpark, J. J. Heyd, E. Brothers, K. N. Kudin, V. N. Staroverov, R. Kobayashi, J. Normand, K. Raghavachari, A. Rendell, J. C. Burant, S. S. Iyengar, J. Tomasi, M. Cossi, N. Rega, J. M. Millam, M. Klene, J. E. Knox, J. B. Cross, V. Bakken, C. Adamo, J. Jaramillo, R. Gomperts, R. E. Stratmann, O. Yazyev, A. J. Austin, R. Cammi, C. Pomelli, J. W. Ochterski, R. L. Martin, K. Morokuma, V. G. Zakrzewski, G. A. Voth, P. Salvador, J. J. Dannenberg, S. Dapprich, A. D. Daniels, O. Farkas, J. B. Foresman, J. V. Ortiz, J. Cioslowski and D. J. Fox, *Gaussian 09, Revision, A.02*, 2009.

76 T. Lu and F. Chen, *J. Comput. Chem.*, 2012, **33**, 580–592.

77 A. Tkatchenko and M. Scheffler, *Phys. Rev. Lett.*, 2009, **102**, 073005.

78 G. Rouillé, C. Jäger, M. Steglich, F. Huisken, T. Henning, G. Theumer, I. Bauer and H.-J. Knölker, *ChemPhysChem*, 2008, **9**, 2085–2091.

79 S. Nakashima, S. Taniguchi, T. Okada, A. Osuka, Y. Mizutani and T. Kitagawa, *J. Phys. Chem. A*, 1999, **103**, 9184–9189.

80 E. R. Johnson, S. Keinan, P. Mori-Sánchez, J. Contreras-García, A. J. Cohen and W. Yang, *J. Am. Chem. Soc.*, 2010, **132**, 6498–6506.

81 J. Contreras-García, E. R. Johnson, S. Keinan, R. Chaudret, J.-P. Piquemal, D. N. Beratan and W. Yang, *J. Chem. Theory Comput.*, 2011, **7**, 625–632.

82 Y. Kai, F. Hama, N. Yasuoka and N. Kasai, *Acta Crystallogr., Sect. B: Struct. Crystallogr. Cryst. Chem.*, 1978, **34**, 1263–1270.

83 J. K. Fawcett and J. Trotter, *Proc. R. Soc. London, Ser. A*, 1965, **289**, 366.

84 J. M. Robertson and J. G. White, *J. Chem. Soc.*, 1945, 607.

85 T. M. Krygowski, M. Cyrański, A. Ciesielski, B. Świrska and P. Leszczyński, *J. Chem. Inf. Comput. Sci.*, 1996, **36**, 1135–1141.

86 B. M. Wong, *J. Comput. Chem.*, 2009, **30**, 51–56.

87 R. A. Marcus, *Rev. Mod. Phys.*, 1993, **65**, 599–610.

88 V. Coropceanu, J. Cornil, D. A. da Silva Filho, Y. Olivier, R. Silbey and J.-L. Brédas, *Chem. Rev.*, 2007, **107**, 926–952.

89 Z. Q. Xie, B. Yang, F. Li, G. Cheng, L. L. Liu, G. D. Yang, H. Xu, L. Ye, M. Hanif, S. Y. Liu, D. G. Ma and Y. G. Ma, *J. Am. Chem. Soc.*, 2005, **127**, 14152–14153.

90 Y. Hong, J. W. Y. Lam and B. Z. Tang, *Chem. Commun.*, 2009, 14152–14153.

91 J.-L. Liao, X. Chen, C.-Y. Liu, S.-A. Chen, C.-H. Su and A.-C. Su, *J. Phys. Chem. B*, 2007, **111**, 10379–10385.

92 Y. Qian, S. Li, G. Zhang, Q. Wang, S. Wang, H. Xu, C. Li, Y. Li and G. Yang, *J. Phys. Chem. B*, 2007, **111**, 5861–5868.

93 D. Kim and J.-L. Brédas, *J. Am. Chem. Soc.*, 2009, **131**, 11371–11380.

94 D. Small, V. Zaitsev, Y. Jung, S. V. Rosokha, M. Head-Gordon and J. K. Kochi, *J. Am. Chem. Soc.*, 2004, **126**, 13850–13858.

95 Z. Xu, N. J. Singh, J. Lim, J. Pan, H. N. Kim, S. Park, K. S. Kim and J. Yoon, *J. Am. Chem. Soc.*, 2009, **131**, 15528–15533.

96 V. Novakova, E. H. Mørkved, M. Miletin and P. Zimcik, *J. Porphyrins Phthalocyanines*, 2010, **14**, 582–591.

97 B. W. Holmes and J. A. R. Griffith, *J. Phys. B: At., Mol. Opt. Phys.*, 1995, **28**, 191.

98 K. Pei, M. Su, L. Chen and X. Zheng, *J. Phys. Chem. B*, 2012, **116**, 7914–7919.

99 T. H. Kim, M. S. Choi, B.-H. Sohn, S.-Y. Park, W. S. Lyoo and T. S. Lee, *Chem. Commun.*, 2008, 2364–2366.

100 V. W.-W. Yam, K. M.-C. Wong and N. Zhu, *J. Am. Chem. Soc.*, 2002, **124**, 6506–6507.

101 S. S. Babu, V. K. Praveen, S. Prasanthkumar and A. Ajayaghosh, *Chem.–Eur. J.*, 2008, **14**, 9577–9584.

102 N. Peimyoo, J. Li, J. Shang, X. Shen, C. Qiu, L. Xie, W. Huang and T. Yu, *ACS Nano*, 2012, **6**, 8878–8886.

103 T. D. Brennan, W. R. Scheidt and J. A. Shelnutt, *J. Am. Chem. Soc.*, 1988, **110**, 3919–3924.

104 L. D. Sparks, W. R. Scheidt and J. A. Shelnutt, *Inorg. Chem.*, 1992, **31**, 2191–2196.

105 S. Nakashima, S. Taniguchi, T. Okada, A. Osuka, Y. Mizutani and T. Kitagawa, *J. Phys. Chem. A*, 1999, **103**, 9184–9189.